2008 IEEE International Conference on
Robotics and Automation
Pasadena, CA, USA, May 19-23, 2008

Dynamics-based Decentralized Control of Robotic Couch and Multi-leaf Collimators for Tracking Tumor Motion

Tarun K. Podder, *Member, IEEE,* Ivan Buzurovic, James M. Galvin, and Yan Yu

Department of Radiation Oncology, Kimmel Cancer Center (NCI-designated)
Jefferson Medical College, Thomas Jefferson University, Philadelphia, PA 19107, USA

Abstract— **Tumors in thorax region incur significant amount of motion and deformation due to respiratory and cardiac cycles. To accommodate this undesired movement, physicians incorporate a large standard margin around the tumor to delineate a Planning Target Volume (PTV), so that the Clinical Target Volume (CTV) receives the prescribed dose under any scenario. Consequently, a large volume of healthy tissue might be irradiated and sometimes it is difficult to spare critical organs adjacent to the tumor. For compensating this tumor motion, techniques such as breath-hold, gating, and Active Tracking and Dynamic Delivery (ATDD) are used. Although, ATDD is the most effective technique, it is the most challenging one. The ATDD can be accomplished in three different ways: adjusting the Multi-Leaf Collimator (MLC), adjusting the couch, and adjusting the MLC and couch simultaneously. The first two techniques have been explored and/or implemented in practice. However, the third approach has not been investigated extensively. In this study, we have proposed a novel approach for ATDD that exploits the advantages of both the MLC (or MLC-bank) and the HexaPOD™ robotic couch. In our proposed new approach, we have decomposed and allocated the tumor motion trajectory to the subsystems (MLC or MLC-bank and HexaPOD™ robotic couch) based on their natural frequency domains using wavelet technique. The efficacy of the proposed method has been investigated by extensive computer simulation and the results are presented in this paper.**

Index Terms – decentralized control, dynamics-based control, frequency decomposition, robotic radiation therapy, robotic couch, multi-leaf collimator, tumor tracking.

I. INTRODUCTION

TUMORS (i.e., target-volumes) in lung, esophagus, pancreas, liver, prostate, breast, and other organs move significantly (upto 4-5cm) during cardiac and respiratory motion [1]-[6]. In order to deliver a prescribed dose to the CTV under any conditions, clinicians delineate PTV with a large margin that can be 5cm or even larger. Consequently, a large volume of healthy tissue is included in PTV and sometimes it is difficult to spare critical organs adjacent to the tumor. Therefore, it is extremely important to irradiate only the target-volume and minimize the healthy tissue irradiation by compensating the tumor movement and deformation. Major factors contributing to the overall geometric error and consequently inaccurate/undesired delivery of radiation dose are: (a) inter- and intra- observer variations in Gross Tumor Volume (GTV) definition, (b) motion artifacts (respiratory and cardiac) on the Computed Tomography (CT) images used to define targets and surrounding structures, (c) motion during dose delivery due to respiration and heartbeat, (d) variations caused by changing organ volumes (e.g., bladder filling during setup and treatment), tumor growth or shrinkage, tissue swelling, and (e) patient setup error. Of these factors, respiratory motion is the major contributor to the target movement and deformation in and around the thorax [1],[6]. It is acknowledged that there are significant motion problems for tumors in the lung, breast, esophagus, liver, and kidney [1]-[9]. However, due to the lack of appropriate technological solutions, it is a common practice to encompass the CTV with a PTV that includes a larger margin to allow for these variations.

Recently, several research groups are investigating various aspects of tumor tracking and developing tools to deliver precise dose to a moving target-volume [5]-[14]. The commonly practiced methods for compensating target/tumor motion are: (i) breath-hold, (ii) gating, and (iii) Active Tracking and Dynamic Delivery (ATDD), however, each technique has its own unique limitations. For example, the MLC gating technique using internal fiducials requires kilovoltage x-ray which delivers unwanted radiation dose to the patient. Additionally, gating suffers from severely low duty-cycle (only 30%-50%) and Intensity Modulated Radiation Therapy (IMRT) has a low efficiency (only 20%-50%). All these factors lead to a 4- to 15-fold increase in delivery time over conventional treatment [6]. Breath-hold techniques require training and are challenging for some patients. Although ATDD can be the most effective technique, it is the most challenging one. The ATDD can be accomplished in three different ways: (1) adjusting the MLC, (2) adjusting the couch, and (3) adjusting the MLC and the couch simultaneously. The first two techniques have been explored and/or implemented in practice, while the third approach has neither been investigated extensively nor been implemented. The commercially available HexaPOD™ robotic couch is capable of positioning the patient more accurately compared to other conventional couches [15], however, currently it does not have provision for compensating the tumor movement that is induced by respiratory and cardiac motions. Recently, a group of researchers has investigated the feasibility of using the treatment couch (HexaPOD™ and Dynatrac) for intra-

Corresponding author: Tarun K. Podder, Thomas Jefferson Hospital, Philadelphia, PA 19107, email: tarun.podder@jeffersonhospital.org.

fraction motion tracking [14]. Such a robotic system which is subjected to a large load and operating at moderate frequency and amplitude requires not only robust electro-mechanical design but also stable closed-loop dynamic control that can produce a high degree of repeatability and accuracy when faced with varying external perturbations.

In this study, we have developed a decentralized closed-loop dynamic controller for adjusting the MLC (or MLC-bank) and robotic couch based on their dynamic response bandwidth so that the tumor-volume appears to be stationary relative to the radiation beam and the beam can be delivered close to 100% duty-cycle. We have also investigated the potential use of a variety different MLC designs for tracking the tumor motion while delivering the radiation beam.

II. MATHEMATICAL FRAMEWORK

A. System Dynamics

We have developed dynamic equations of motion for the HexaPOD™ robotic couch, which is a special type of Stewart Platform, i.e., a parallel robotic manipulator (Fig. 1) using Lagrangian formulation [16]-[17]. The Lagrangian function of a dynamic system can be expressed as:

L = Kinetic energy (K) – Potential energy (P) (1)

Thus, the general form of dynamic equations is

$$\frac{d}{dt}\left(\frac{\partial L}{\partial \dot{q}}\right)-\frac{\partial L}{\partial q}=\tau \quad (2)$$

where, $q \in R^n$ is the vector of generalized coordinates, and τ is the generalized force (or torque) applied to the system through the actuators.

In our study, we have used the following notations for modeling the HexaPOD™, i.e. the Stewart platform. Referring Fig. 1(a), (b)& (c), we have assigned an inertial frame (X,Y,Z) at the center O of the lower platform, i.e. the BASE, and assigned another moving coordinate system (x,y,z) at the center of the top platform, i.e. the TOP. The BASE frame is assigned and called as fixed frame and the TOP frame is moving and is called as moving frame.

To specify the configuration of the 6DOF Stewart Platform, six independent position-orientation variables are needed. Denote the position of the origin of the TOP frame with respect to the BASE frame $[p_x \quad p_y \quad p_z]^T$. The orientation is not defined by the standard Euler angles, but by rotating the TOP frame first about the fixed X-axis by α, then about fixed Y-axis by β and finally about Z-axis by γ. We denote $R_X(\alpha)$, $R_Y(\beta)$ and $R_Z(\gamma)$ as the three matrices that represent three basic rotations as follows:

$$R_X(\alpha)=\begin{bmatrix}1 & 0 & 0\\ 0 & C\alpha & -S\alpha\\ 0 & S\alpha & C\alpha\end{bmatrix},\ R_Y(\beta)=\begin{bmatrix}C\beta & 0 & S\beta\\ 0 & 1 & 0\\ -S\beta & 0 & C\beta\end{bmatrix},\ R_Z(\gamma)=\begin{bmatrix}C\gamma & -S\gamma & 0\\ S\gamma & C\alpha & 0\\ 0 & 0 & 1\end{bmatrix}$$

where C(.) =cos(.), and S(.) = sin(.). This definition of the orientation not only provides us with a clear physical meaning but also avoids violating the one-to-one relationship between the system configuration and the values of X_{p-o}, which may cause the Jacobian matrix to lose its rank, even if the system is not in a singular configuration. Thus, the position and orientation of the upper platform is specified by the Cartesian coordinate system as $X_{p-o}=[p_x, p_Y, p_Z, \alpha, \beta, \gamma]^T$.

Now, the dynamic equations in Cartesian-space (or task-space) are expressed as-

$$M(X_{p-o})\ddot{X}_{p-o}+V_m(X_{p-o},\dot{X}_{p-o})\dot{X}_{p-o}+G(X_{p-o})=J^T(X_{p-o})F_{td} \quad (3)$$

where, $F_{td}=(f_1,f_2,f_3,f_4,f_5,f_6)$ is the vector of forces applied by the actuators of the legs, J is the full system Jacobian matrix.

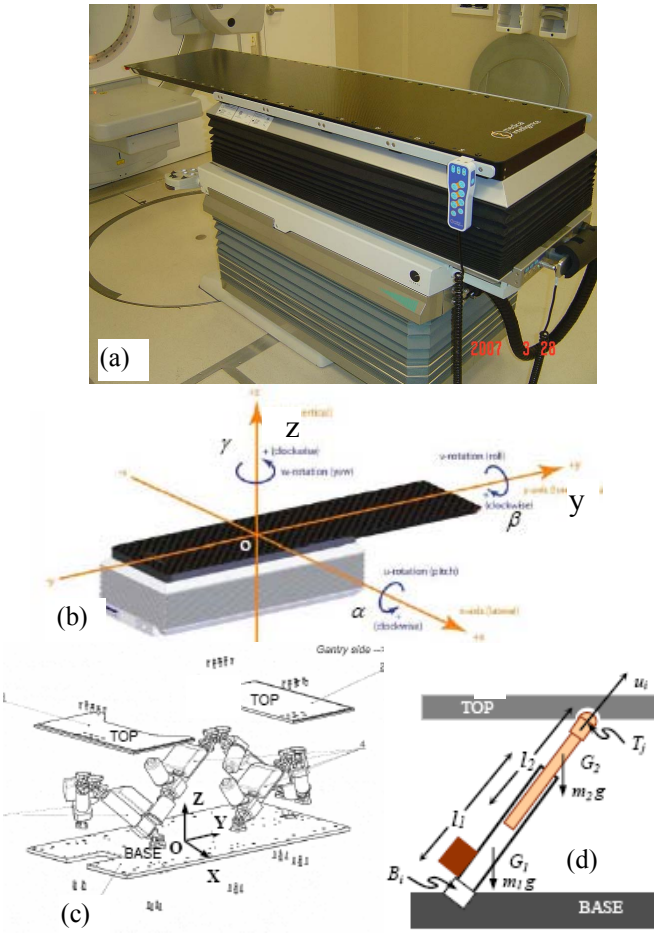

Fig. 1. HexaPOD™ robotic couch, (a),(b) external isometric view, (c) internal isometric view, and (d) schematic of the leg.

For convenience, we divide the HexaPOD™ robotic couch into two subsystems: the upper platform (TOP) and the six legs (Fig. 1). We compute the kinetic energy and potential energy of these subsystems and then derive the global dynamic equations.

Kinetic and Potential energies

Kinetic energy of the upper platform

$$K_{up}=K_{up(trans)}+K_{up(rot)}=\frac{1}{2}m_u(\dot{p}_X^2+\dot{p}_Y^2+\dot{p}_Z^2)+\frac{1}{2}\Omega_{up(mf)}^T I\,\Omega_{up(mf)} \quad (4)$$

Potential energy of the upper platform:

$$P_{up} = m_u g\ p_Z \tag{5}$$

Kinetic energy of the legs:

$$K_{L_i} = \frac{1}{2}(m_1 + m_2)[h_i V_{T_j}^T V_{T_j} - k_i V_{T_j}^T (u_i)(u_i)^T V_{T_j}] \tag{6}$$

where, L_i is the length of the leg at the current configuration, $(m_1 + m_2)$ is the mass of the leg, V_{T_j} is the velocity of the leg, and

$$h_i = \left(\frac{\hat{l}}{L_i} + \frac{m_2}{m_1 + m_2}\right)^2, \hat{l} = \frac{\delta m_1 - \frac{1}{2} m_2 l_2}{m_1 + m_2}, k_i = h_i - \left(\frac{m_2}{m_1 + m_2}\right)^2 \tag{7}$$

Potential energy of the legs:

$$P_{Legs} = (m_1 + m_2) g \sum_{i=1}^{3} \left[\hat{l}\left[\frac{1}{L_{2i}} + \frac{1}{L_{2i-1}}\right] + \frac{2m_2}{m_1 + m_2}\right](p_Z + Z_{T_i}) \tag{8}$$

where, $Z_{T_j} = [0 \quad 0 \quad 1][R_Z(\gamma)^T R_X(\alpha)^T R_Y(\beta)^T GT_{j(mf)}]$; $GT_{j(mf)}$ is obtained from the geometry of the platform. Substituting the expression from equations (4)-(8) into equations (1), and (2), we can obtain the dynamic equations of the form (3) for the the HexaPOD (leg plus top platform). Recalling equation (3), more precisely we can write,

$$\left.\begin{aligned} &M(X_{p-o}) = M_{up} + M_{Legs}, V_m(X_{p-o}, \dot{X}_{p-o}) = V_{m_{up}} + V_{m_{Legs}}, \\ &G(X_{p-o}) = G_{up} + G_{Legs} \end{aligned}\right\} \tag{9}$$

The MLC was modeled as mass-spring-damper system considering the mass moving in the horizontal plane. The dynamic equation for MLC is as follows:

$$M_{MLC}\ \ddot{x} + C_d\ \dot{x} + K_s\ x = F_{MLC} \tag{10}$$

where, M_{MLC} is the mass, x is the position, $\dot{x}$ is the velocity, $\ddot{x}$ is the acceleration, C_d is the damping constant, K_s is the spring constant and F_{MLC} is the force of the MLC.

The dynamic equations of motion for HexaPOD™ robotic couch and the MLC have been discussed above. These equations are essential in developing our proposed dynamics-based coordinated control system (Fig. 2).

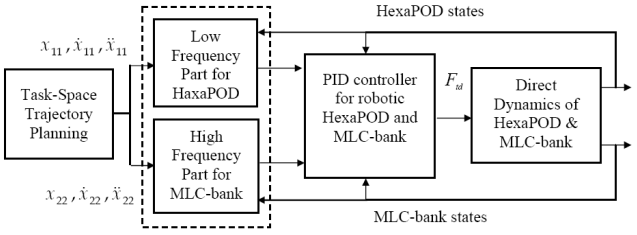

Fig. 2. Block diagram of the decentralized coordinated dynamics-based closed-loop controller for HexaPOD robotic couch and linear accelerator's MLC-bank.

B. Control scheme

To track the tumor trajectory for optimal dose delivery to the CTV while sparing normal tissue, we propose to control both the MLC (MLC-bank) and the HexaPOD™ simultaneously [19]-[21]. Thus, we have two subsystems (MLC or MLC-bank and HexaPOD™ couch) with vastly different dynamic responses, i.e., natural frequency bandwidths. In the proposed approach, the trajectory of the tumor movement due to respiratory and cardiac motions is decomposed into two segments (high and low frequency segments) using the Wavelet technique or Fourier series. The high frequency component is assigned to the lighter subsystem, i.e. the MLC or MLC-bank, and the low frequency segment is allocated to the heavier subsystem, i.e. the couch (Fig. 2).

To implement the proposed algorithms, we have used a Proportional, Integral and Derivative (PID) control scheme. Dropping the subscripts, we can rewrite equation (3) as

$$M(X)\ddot{X} + \xi(X, \dot{X}) = \Im \tag{11}$$

where, $\xi(X, \dot{X}) = V(X, \dot{X})\dot{X} + G(X)$, and $\Im = J^T(X_{p-o})F_{td}$.

Now, we write the computed torque as follows-

$$\hat{M}[\ddot{X}_d + K_V(\dot{X}_d - \dot{X}) + K_P(X_d - X)] + \hat{\xi} = \Im \tag{12}$$

where, $\hat{M}$ and $\hat{\xi}$ are the estimates of the system's model parameters, $K_V = diag(k_{v1}, k_{v2}, \cdots, k_{v6})$ is the derivative gain matrix and $K_P = diag(k_{p1}, k_{p2}, \cdots, k_{p6})$ is the proportional gain matrix.

If the estimates of the model parameters are close approximation of the actual system's parameters, from equations(11) and (12) we can write,

$$\ddot{X} = \ddot{X}_d + K_V(\dot{X}_d - \dot{X}) + K_P(X_d - X) \tag{13}$$

Now, denoting the position, velocity, and acceleration errors as $e = X_d - X$, $\dot{e} = \dot{X}_d - \dot{X}$, $\ddot{e} = \ddot{X}_d - \ddot{X}$, we can rewrite equation (13) as

$$\ddot{e} + K_V\dot{e} + K_P e = 0 \tag{14}$$

The equation (14) guarantees asymptotic reduction of the tumor tracking errors. However, to reduce any steady-state errors, we also incorporate an integral control part into equation (14), thus the final control equation becomes,

$$\ddot{e} + K_V\ \dot{e} + K_P\ e + K_I \int_0^t e\ dt = 0 \tag{15}$$

where, K_I is the integral gain. Thus, equation (15) ensures asymptotic decay of the transient errors as well as reduction of steady-state errors.

C. Trajectory generation

Assuming a fixed period for the motion, we have chosen the position of the tumor as a function of time in parametric form as follows [17]:

$$y(t) = y_0 - b\cos^{2n}\left(\frac{\pi t}{T} - \phi\right) \tag{16}$$

where y_0 is the position at exhale, b is the extent (amplitude) of the motion, T is the period of breathing cycle, n is a parameter that determines the general shape (steepness and flatness) of the model, and ϕ is the initial phase of the breathing cycle. To make the simulation more realistic, we have modified equation (16) by incorporating a high frequency component and a random noise function as given by the equations (17) and (18) below.

$$y_1(t) = y_1 - b_1\cos\left(\frac{\pi t}{mT} - \phi_1\right) \tag{17}$$

$$y_d(t) = c\ rand(c_1, t) - \frac{c}{2}; \quad c,\ c_1 \text{ are constants} \qquad (18)$$

Thus, the resultant function of the tumor motion in patient's superior-inferior direction becomes as follows:

$$s(t) = y(t) + y_1(t) + y_d(t) \qquad (19)$$

Using wavelet technique (available in MATLAB), we decomposed the equation (19) into two segments as

$$s(t) = a_1(t) + d_1(t) \qquad (20)$$

where $a_1(t)$ was the low frequency component that was allocated to the HexaPOD^{TM} couch and $d_1(t)$ was the high frequency component that was allocated to the MLC (Fig. 2 and Fig. 3).

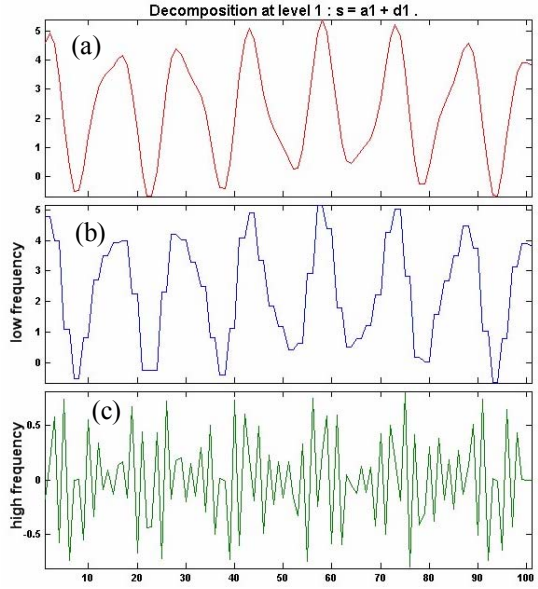

Fig. 3. Wavelet decomposition of the tumor motion, (a) resultant motion, (b) low frequency component, and (c) high frequency component.

III. Case Study

We have investigated three different schemes for tracking the tumor trajectory and compared our proposed approach (approach C) with two other methods (approaches A & B) that have been explored by several researchers. These three approaches are explained below.

A. MLC only (2D tracking)

We investigated a variety of MLC and MLC-bank designs for tracking tumor motion. In this case, the HexaPOD^{TM} remained stationary during the course of radiation delivery. The MLC (or MLC-bank) can be moved in 2-dimensional plane (1.5D to be more precise; because the individual MLC is 0.3-1cm thick in the perpendicular to radiation beam direction). Thus, with MLC (or MLC-bank) one will be able to track the tumor motion maximum in two directions (or 1.5D). However, for optimal delivery of radiation to the CTV, it is important to track the tumor at least in 3D, i.e. superior-inferior, anterior-posterior and left-right directions of the patient; rotational tracking may not be critical for most patients.

B. HexaPOD^{TM} only (3D tracking)

In this case, we deploy the HexaPOD^{TM} robotic couch to track the tumor motion in 3D (3 positions (x,y,z) and 3 orientations (about x, y & z axes)). In this case, MLCs are used in a conventional way to deliver IMRT, or 3D conformal radiation therapy can be applied for treating the patient. It is to be noted that in this case the MLC is not used to track the tumor motion.

C. HexaPOD^{TM} and MLC (3D finer tracking)

We have investigate the efficacy of the proposed decentralized dynamics-based control strategy as depicted in Fig. 2 by using both the MLC (MLC-bank) and the HexaPOD^{TM} robotic couch. Although, the HexaPOD^{TM} may be able to track the tumor in all 6DOF, it may be difficult to move the couch with a heavy payload with high frequency and consequently may incur more errors in tracking and may require very large actuation force. Therefore, in our proposed approach the high frequency movement is allocate to the MLC and the low frequency motion is assigned to the couch.

Simulation parameters

For the computer simulation, we have considered predominating direction (superior-inferior direction) of the lung tumor motion. We have taken mass of the couch top = 14kg, mass of the leg =5kg, length of the leg =20cm, mass of the MLCs = 0.5, 1, 5, 10 20, 40 80kg, mass of the patient (payload) = 180kg. Parameters for the breathing function are: $y_0 = 0$, $T = 3.0$sec, $b = 4.6$cm, $n = 1$, $m = 5.23$, $b_1 = 0.1$, c = 0.2, c1 = 1, $y_1 = 0$, $\phi_1 = 0$ and $\phi = 0$, , sampling frequency = 5Hz, and total time of simulation (t) = 20sec.

IV. Results and Discussion

The computer simulation results for all three cases namely *MLC only*, *HexaPOD^{TM} only* and *HexaPOD^{TM} plus MLC* are presented in the Fig. 4 through Fig. 15 below.

A. MLC only

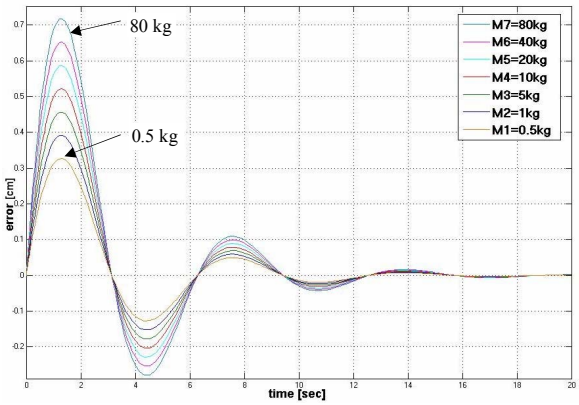

Fig. 4. Tumor tracking errors – using MLCs (or MLC-banks) with different masses (from 0.5kg to 80kg) for MLC only case.

It was observed that the initial tracking errors are less for smaller MLC masses (Fig. 4). However, as time progressed the errors gradually reduced close to zero. This simulation

shows that smaller MLCs could be more effective in tracking the tumor motion promptly. This is because of the fact that the heavier MLCs had larger inertias which required some time to follow the tumor trajectory. These added inertias, system friction and damping gave rise to the actuation forces (as shown in Fig 6). However, the velocities were similar for all the MLCs irrespective of their masses (Fig. 5). Since the amplitude and frequency of the breathing function is quite practical [1]-[5], these velocities would be required to track the tumor in time and space. However, MLCs currently available MLCs on most commercial linear accelerators may not be able to produce such velocities (maximum 3.9cm/sec [23]). Thus, to cover all types of patients it may be required to design a new MLC or to modify the existing MLC systems.

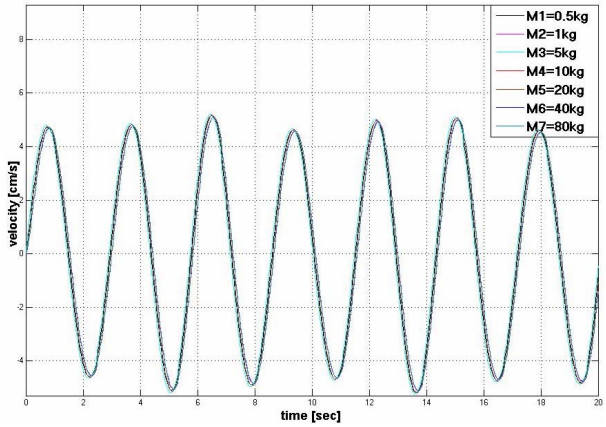

Fig. 5. Velocity of the MLCs (or MLC-banks) for MLC only case.

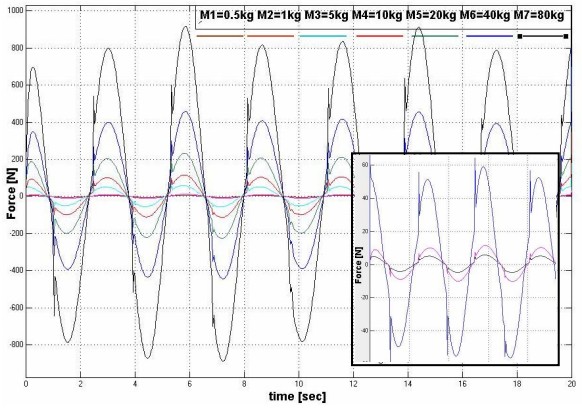

Fig. 6. Actuation force for the MLCs (or MLC-banks) for MLC only case. Inset shows the zoomed-in view of the forces for 0.5, 1 & 5kg MLCs.

B. HexaPOD™ only

We observed about ±0.2cm error (Fig. 7) when the tumor trajectory was tracked using HexaPOD™ couch only. This might be due to high frequency sinusoidal function and random function incorporation with the regular breathing function, which the couch could not follow accurately. However, the velocity (Fig. 8) was similar to MLC velocity (Fig. 5), which was required to track the tumor. The actuator forces are shown in Fig. 9, where four legs shared the main load that was required for superior-inferior (y-direction) motion.

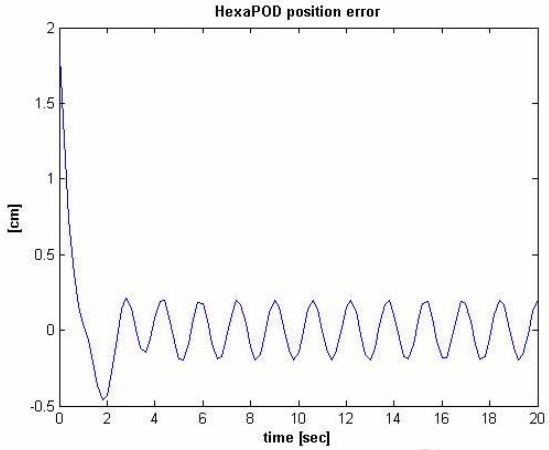

Fig. 7. Tumor tracking errors when only HexaPOD™ is deployed.

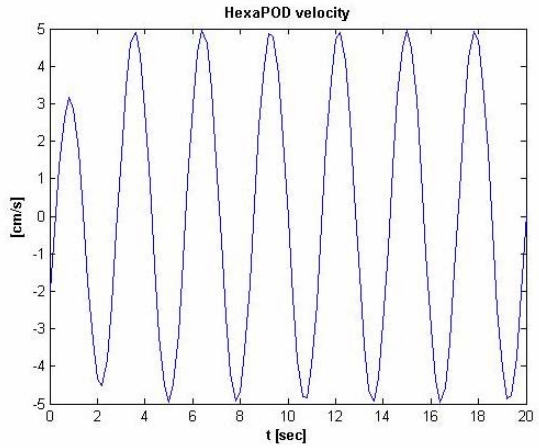

Fig. 8. Velocity of the HexaPOD™ robotic couch when only it is used.

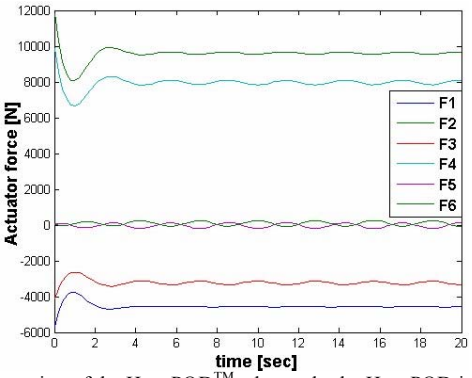

Fig. 9. Actuation of the HexaPOD™ when only the HexaPOD is used for tracking the tumor motion.

C. HexaPOD™ and MLC

We observed significant improvement in tumor tracking while the decomposed trajectories were allocated to both the MLC and the HexaPOD™ couch (Fig. 10). In comparison, we noticed large residual fluctuating error in tumor tracking when only the HexaPOD™ couch was used (Fig. 7) or larger

errors when only the MLC (MLC-bank) was used. Displacement, velocity and acceleration of both the subsystems, i.e. the MLC (1kg) and the HexapOD^{TM} couch are presented in Figs. 11, 12 and 13. We noticed smaller but high frequency movement of MLC as compared to HexaPOD^{TM}; they shared the task-space tracjectory i.e. the tumor motion in such a way so that the agile MLC could trace the high frequency part more effectively. The MLC velocity was about 3.7cm/sec, which can be achieved by the currently available linac machines (Fig. 12). The spikes in MLC's acceleration profile are indicative of the high frequency random noise (Fig. 14). The operating forces and torques are presented in Fig. 15. Although, like the previous case (HexaPOD^{TM} only), the large forces are shared by four legs for one dimensional superior-inferior motion, the magnitude of these forces is one order less than the previous case and thus, would require smaller motors. This happened due to the avoidance of high frequency portion of the trajectory which was allocated to the MLC. Thus, it appears that our proposed decentralized dynamics-based controller could track the tumor motion more accurately compared to other two approaches (MLC only case and HexaPOD^{TM} only case).

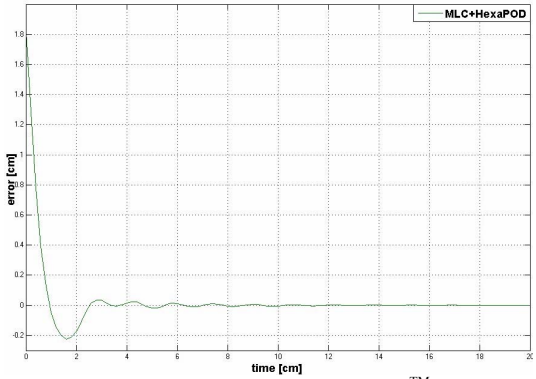

Fig. 10. Tumor tracking errors when both the HexaPOD^{TM} and the MLC are deployed to track the tumor motion.

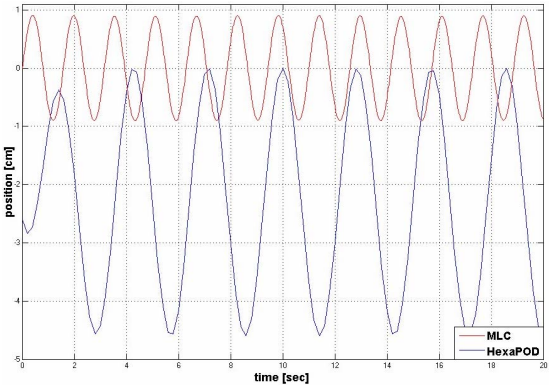

Fig. 11. Displacement of the HexaPOD and the MLC.

Moreover, the MLC can be used for only 1.5D/2D motion tacking. Whereas, the HexaPOD^{TM} can be used for 3D motion tracking. However, the MLC and HexaPOD^{TM} combination can track any tumor trajectory not only in 3D, but also with improved accuracy and reduced actuation force

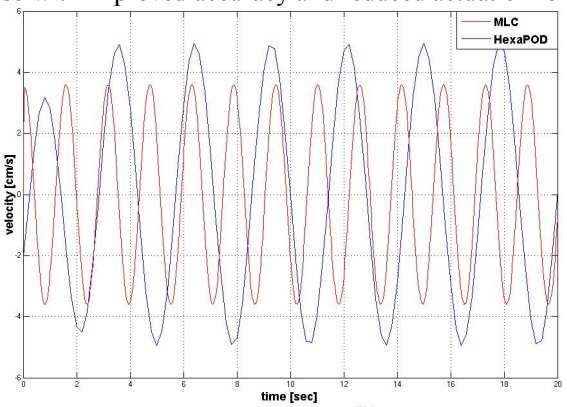

Fig. 12. Velocity of the HexaPOD^{TM} and the MLC.

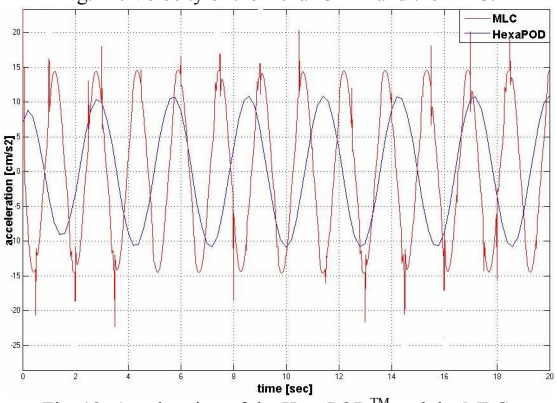

Fig. 13. Acceleration of the HexaPOD^{TM} and the MLC.

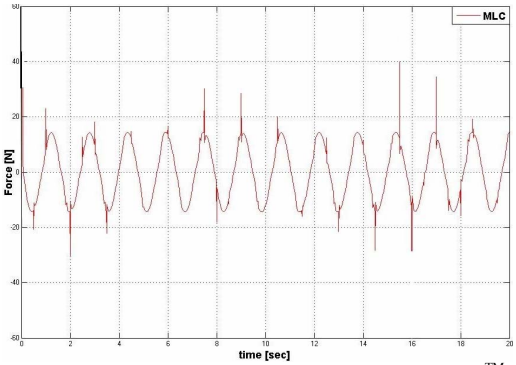

Fig. 14. Actuation of the MLC when both MLC and HexaPOD^{TM} are used for tracking the tumor.

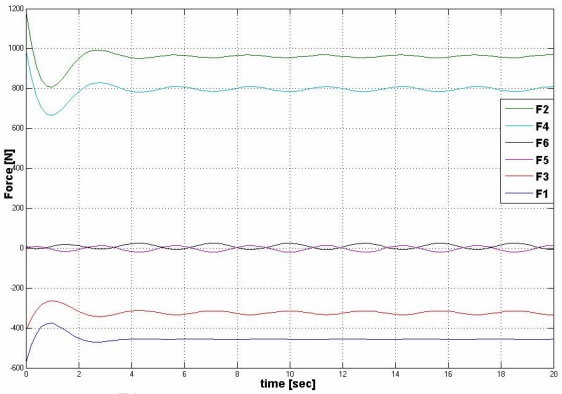

Fig. 15. HexapPOD^{TM} operating forces and torques when both MLC and HexaPOD are used to track the tumor.

V. Conclusion and Future Work

In this paper, we presented a novel decentralized dynamics-based planning and control approach for tumor tracking during radiation therapy. The proposed method was compared with two other methods that are available in the literature. From the simulation results it appeared that our proposed method could yield superior tracking of the tumor motion induced by respiratory (and/or cardiac) motion. Implementation of the proposed technique can potentially improve real-time tracking of the tumor-volume to deliver precise radiation dose at almost 100% duty cycle while minimizing irradiation to health tissues and sparing critical organs. This, in turn, will potentially improve the quality of patient treatment by lowering the toxicity level and increasing survival. In the proposed method, velocity of the MLC was within the capability of the currently available machines for covering all types of patients; and the required actuation forces for the HexaPOD^{TM} were much smaller. In this study, we have deployed a relatively simple closed-loop PID control. Subsequently, we will be investigating the efficacy of the adaptive control and optimal control (if necessary). Adaptive control can be a good choice because of the variability in the payload on the system, i.e., the weight of the patient. One of the main challenges is to synchronize the respiratory motion with the robotic couch and/or IMRT delivery (or 3D conformal radiotherapy) considering the target-volume deformation in addition to target movement. Here we have presented the simulation results for dominating direction of target motion, i.e. superior-inferior direction of the patient. However, the mathematical framework and proposed method can be used for 3D motion of the target. We are working on these aspects of the study. To optimize the computational time and to improve system's response, we will also investigate the use of reduce order dynamic equations and dynamic system identification method.

References

[1] S. Hiroki, S.K. Suzuki, G.C. Sharp, *et al*., "Speed and amplitude of lung tumor motion detected in four-dimensional setup and in tumor-tracking radiotherapy", Int. J. Radiation Oncology Biol. Phys., Vol. 64, No. 4, pp. 1229–1236, 2006.

[2] Q. S. Chen, M. S. Weinhous, F. C. Deibel, J. P. Ciezki, and R. M. Macklis, "Fluoroscopic study of tumor motion due to breathing: Facilitating precise radiation therapy for lung cancer patients," Med. Phys. , 28(9), 1850–1856, 2001.

[3] E. A. Barnes, B. R. Murray, D. M. Robinson, L. J. Underwood, J. Hanson, and W. H. Roa, "Dosimetric evaluation of lung tumor immobilization using breath hold at deep inspiration," Int. J. Radiat. Oncol., Biol., Phys. 50(4), 1091–1098, 2001.

[4] S.C. Erridge, Y. Seppenwoolde, S.H. Muller, M. van Herk, K. De Jaeger, J.S. Belderbos, L.J. Boersma, and J.V. Lebesque, "Portal imaging to assess set-up errors, tumor motion and tumor shrinkage during conformal radiotherapy of non-small cell lung cancer," Radiother. Oncol. 66(1), 75–85, 2003.

[5] C. Ozhasoglu, and M.J. Murphy, "Issues in respiratory motion compensation during external-beam radiotherapy," *Int. J Radiat Oncol Biol Phys* 52(5):1389–1399, 2002.

[6] P.J. Keall, G.S. Mageras, J.M. Balter, et. al. "The management of respiratory motion in radiation oncology report of AAPM Task Group 76", in the *J. Medical Physics*, Vol. 33, No. 10, pp. 3874-3900, 2006.

[7] G. Benchetrit, "Breathing pattern in humans: diversity and individuality," *Respir Physiol* 122(2-3):123–129, 2000.

[8] S.S. Vedam, P.J. Keall, A. Docef, D.A. Todor, V.R. Kini, and R. Mohan, "Predicting respiratory motion for four-dimensional radiotherapy." in the *J. Medical Physics,* Vol. 31, No. 8, pp. 2274–2283, 2004.

[9] G.C. Sharp, S.B. Jiang, S. Shimizu, and H. Shirato, "Prediction of respiratory tumour motion for real-time image-guided radiotherapy," in the *J.Phys Med Biol*. Vol. 49, No. 3, pp. 425–440, 2004.

[10] A. Schweikard, G. Glosser, M. Bodduluri, M. J. Murphy, and J. R. Adler, "Robotic motion compensation for respiratory movement during radiosurgery," in the *Comput Aided Surg* 5(4):263–277, 2000.

[11] Y. Kamino, K. Takayama, M. Kokubo, *et al*. "Development of a four-dimensional image-guided radiotherapy system with a gimbaled x-ray head", Int. J. Radiation Oncology Biol. Phys., Vol. 66, No. 1, pp. 271–278, 2006.

[12] W. D'Souza, and T.J. McAvoy, "Analysis of the treatment couch and control system dynamics for respiration-induced motion compensation", in the *J. Medical Physics*, Vol. 33, No. 12, pp. 4701-4701, 2006.

[13] P.J. Keall, H. Cattell, D. Pokhrel, et al., "Geometric accuracy of a real-time target tracking system with dynamic multileaf collimator tracking system", in the *Int. J. Radiation Oncology, Biology and Physics*, Vol. 65, No. 5, pp. 1579-1584, 2006.

[14] W. D'Souza, S.A. Naqvi, and C.X. Yu, "Real-time intra-fraction-motion tracking using the treatment couch: a feasibility study", in *Phys. Med. and Bio.*, Vol. 50, pp. 4021-4033, 2005.

[15] H. Chung, T. Jin, T. Suh, J. Palta, and S. Kim, "Mechanical accuracy of a robotic couch," in the journal *Medical Physics*, Vol. 33, No. 6, pp. 2041, 2006.

[16] J.J. Craig, "*Introduction to Robotics"*, Addison-Wesley, New York, 1989.

[17] G. Lebret, K. Liu, and F.L. Lewis, "Dynamic analysis and control of a Stewart platform manipulator," in the *J. Robotic Systems*, Vol. 10, No. 5, pp. 629–655, 1993.

[18] A.E. Lujan, E.W. Larsen, J.M. Balter, and R.K. Ten-Haken, "A method for incorporating organ motion due to breathing into 3D dose calculations", in the *J. Medical Physics*, Vol. 26, No. 5, pp. 715-720, 1999.

[19] T.K. Podder, and N. Sarkar, "Dynamic trajectory planning for autonomous underwater vehicle-manipulator systems", in the *Int. Conf. on Robotics and Automation (ICRA)*, pp. 3461-3466, San Francisco, 2000.

[20] T.K. Podder and N. Sarkar, "*Unified Dynamics-based Motion Planning Algorithm for Autonomous Underwater Vehicle-Manipulator Systems (UVMS)*," in the book entitled "*Mobile Robots - Moving Intelligence*", edited by Jonas Buchli (ISBN: 3-86611-284-X), Chapter 15, pp. 321-356, December 2006.

[21] T.K. Podder, I. Buzurovic, and Y. Yu, "Coordinated dynamics-based control of robotic couch and MLC-bank for feedforward radiation therapy", in the *Journal Computer Assisted Radiology and Surgery*, Vol. 2, pp. S49-52, June 2007.

[22] P. Liang, J.J. Pandit, and P.A. Robbins, "Non-stationarity of Breath-by-Breath Ventilation and Approaches To Modeling the Phenomenon," in the *Modeling and Control of Ventilation*. S. J. G. Semple, L. Adams, and B. J. Whipp (eds.). New York: Plenum Press, pp. 117–121, 1995.

[23] K. Wijesooriya, C. Bartee, J.V. Siebers, S.S. Vedam, and P.J. Keall, "Determination of maximum velocity and acceleration of a dynamic multileaf collimator: implications for 4D radiotherapy", *Medical Physics*, Vol. 32, No. 4, pp. 932-941, 2005.